SLJoAS Sri Lankan Journal of Applied Sciences

Research Article

Optical Nonlinearity and Enhanced Second Harmonic Generation in Copper–doped Cadmium Iodide Nanocrystals

M. Idrish Miah
Department of Physics, University of Chittagong, Chittagong–4331, Bangladesh.

*** Corresponding author email address**: m.idrish.miah@cu.ac.bd

(Received 5th April 2025; Accepted 26th May 2025)

Abstract

Cadmium iodide nanocrystals are grown and doping defect and quantum-confinement effects in optical susceptibility in the nanocrystals are investigated. The nanomaterials with various crystal sizes are pumped with intense laser beams. This pump-probe experiment probes the doubled-frequency second harmonic generation (SHG). The second–order optical susceptibility is calculated from the experimentally measured SHG intensity. The results show that a significant enhancement in the optical susceptibility is achieved in nanomaterials with moderate doping. However, bulk and intrinsic crystals show no considerable SHG effect. The results were discussed within models of the impurity induced metallic-aggregators and photoinduced electron-phonon anharmonic interactions.

Keywords: Nanomaterials; Nano-confined effect; Doping effect; Optical susceptibility

1. Introduction

Because the progress of photonics and optoelectronics has been built on the optical nonlinear properties of materials, optical nonlinear materials have been investigated from the point of view of nonlinear quantum processes and their potential in applications in photonics such as optical switching, transmission, optical communications, amplification and optical power limiting, optical filters or sensor protections [1].

Multiphoton spectroscopy [2], multiphoton spin spectroscopy [3] and the second harmonic generation (SHG) [4] in materials have widely been used to study the higher-order optical nonlinear processes. Of them, the SHG is an important technique to investigate the nonlinear optical processes, particularly, the surface effects of a material. As the surface-to-volume ratio of a material in nano-structures is larger than that in the bulk, the surface effects of the nonlinearities play a vital role in nanomaterials.

Because the SHG is prevented by symmetry in a centrosymmetric material, one needs to form noncentrosymmetric process in order to observe the SHG. However, there are some possibilities of breaking this property by means of inducing the noncentrosymmetricity in the crystals [5,6]. For example, this property is generally broken at the surface of a material since that region no longer presents an inversion centre. This very special property is what enables second-order nonlinearities to be so effective for surface and interface measurements. Likewise, any other mechanisms that break the symmetry, such as an electric field/mechanical stress, inserting suitable impurities into the crystal, reducing the size of the crystals, or lowering the crystal temperature, may also allow a second-order signal to be produced for the observation of the SHG [7,8].

Cadmium iodide (CdI_2) single crystals are indirect and wide-band gap semiconductors having layered structure [7]. Bulk crystals CdI_2 are symmetric. Recent research records in the literature show that bulk CdI_2 process higher-order optical nonlinearities [9-12]. The band structure calculations of the CdI_2 crystals have also shown a large anisotropy in the space charge density distribution causing high anisotropy in the corresponding optical spectra. The anisotropic behaviour of the CdI_2 crystals favours the local noncentrosymmetry [7,13]. It makes CdI_2 nanocrystals promising and motivates the present research.

A preliminary study was conducted on the photoinduced SHG in copper-doped cadmium iodide single crystals [14], where they found the maximum SHG effect for the copper content of about 0.4%, but they did not systematically study the doping dependence. The photoinduced electron-phonon anharmonic interactions in the copper-doping responsible for the enhanced SHG effect were explored in [4]. It was shown that the local hyperpolarizability for the copper aggregates as well as the corresponding nonlinear susceptibility played the crucial role in the SHG effect in centrosymmetric systems. Recently, we experimentally introduced novel processes of inducing the noncentrosymmetricity in centrosymmetric nonlinear optical nanocrystal systems [8], where the involvement of the interlayer phonons for the photoinduced electron-phonon anharmonic interactions was also confirmed by the observation of the low-frequency phonon modes in Raman spectrum. In this paper, the power dependence as well as the intrinsic and thick crystals were not studied. Here, in the

present study, we include these and extend our investigation. The output SHG signal is measured from the crystals with various sizes and doping, pumped with an intense laser with different powers. The second–order optical susceptibility is calculated from the measured SHG signal. A significant enhancement in the optical susceptibility is achieved in the thin nanocrystals compared to that in the intrinsic or thick crystals. We then explore the doping defect and nano-confined effects in the optical susceptibility of the materials. This is the first report on such study.

2. Experimental

Copper-doped cadmium iodide (Cu-CdI_2) nanocrystals were synthesized from the mixture of cadmium iodide (CdI_2) and cuprous oxide (CuI) using a standard method [15]. Structure was monitored using the Ultima IV X-ray diffractometer and tunnelling electron microscope. The grown nanocrystal sizes were from sub-nm to 100 nm. The optical bandgap (E_g) of the crystals was estimated from an indirect-type transition and from fittings to the low and high wavelength regions of the absorbed photon energy curve and using the relation for the indirect E_g [16]. The average value of E_g was found to be 3.65 eV. The investigations were performed at pump-probe conditions and at low temperatures by mounting the samples in a temperature-regulated cryostat. We used an Nd laser as a fundamental laser for the SHG measurements. The laser generates ps pulses (of average peak power of 15 mW) having a repetition rate of 80 Hz. The output SHG signal at 530 nm and the fundamental signal at 1064 nm were spectrally separated by a monochromator showing spectral resolution of about 5 nm mm^{-1}. Detection of the doubled-frequency (within green spectral region) output SHG signal was performed by a photomultiplier equipped with an electronic boxcar integrator for registration of the output. A scheme of the experimental setup, similar to that in [4], is shown in Figure 1.

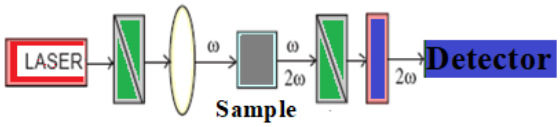

Fig.: 1. A scheme of the experimental setup for the measurements. The fundamental light beam goes to the sample through the polarizer and lens. It is then spectrally separated by a monochromator for the detection by a photomultiplier (Detector) equipped with an electronic boxcar integrator.

The second-order susceptibility $\chi^{(2)}$ for samples with different thickness T was calculated from the experimentally measured SHG using the following expression for the SHG intensity [4]:

$$I(2\omega,t)=\frac{2\mu_0^{3/2}\omega^2T^2\zeta^2(\chi^{(2)})^2I^2(\omega,t-\Delta t)}{\pi\in_0^{3/2}R^2n(2\omega)n^2(\omega)},$$

where R is the radius of the pumping beam which possesses a Gaussian-like form, T is the length of the nonlinear medium (thickness of the crystal), μ_0 and $\in_0$ are the static (low-frequency) values of the magnetic permeability and the electric permittivity respectively, $n(\omega)$ and $n(2\omega)$ are the refractive indices for the pumping and the SHG doubled frequency respectively, and

$$\zeta=\frac{\sin T\Delta k(t)/2}{T\Delta k(t)/2},$$

where $\Delta k=k(2\omega)-2k(\omega)$ is the phase matching wave vector defined by optical birefringence.

3. Results

The doubled-frequency SHG signal as a function of the time delay between the pump and probe is shown in Fig. 2. This delay dependence in the second harmonic signal shows a relatively large relaxation time, which demonstrates the principal role of long-lived electron–phonon states in the observed effects. This can be explained within a model of the photo-induced electron-phonon anharmonicity [4], where the relaxation time for the nanolayers should be larger than for the strong localized electron–phonon states due to the nanosize-confined effect.

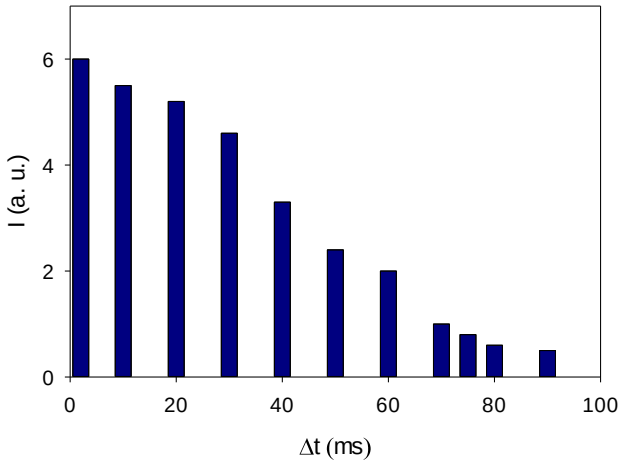

Fig. 2: SHG signal as a function of the time delay between the pump and probe beams for a 0.6% copper-doped nanocrystal with thickness 3.5 nm.

Figure 3 shows the pump power (P) dependence of the second harmonic signal for various thicknesses of the nanocrystals at liquid nitrogen temperature. As can be seen, the signal increases with decreasing the thickness T of the nanocrystals. This dependence shows a beginning of slight preserved and is increased before reaching the value a little higher than the background signal. The background signal is obtained for the intrinsic CdI_2 crystals or the bulk. However, a significant enhancement in the signal occurs for the thinnest nanocrystals at a power of 24 GW/m^2. The secondary maximum seems to be shifted in the higher pump power with decreasing thickness of the nanocrystals. The qualitative and quantitative changes that occurred for the thinner nanocrystals correspond to the manifestation of the

quantum-confined excitonic levels perpendicularly to the layers.

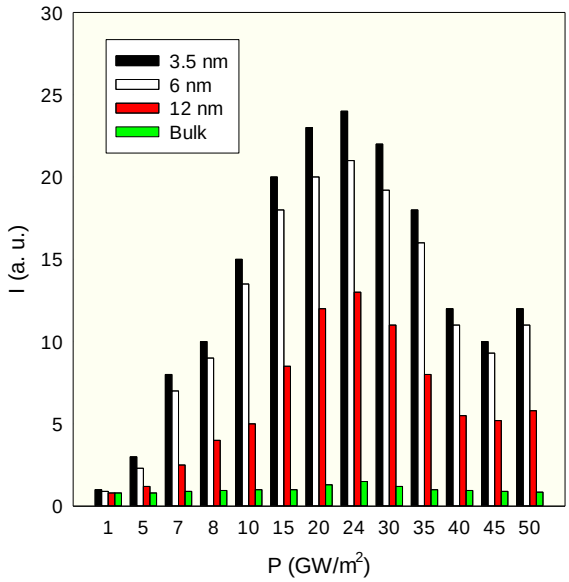

Fig.3: SHG signal as a function of pumping power. The background signal is for the bulk crystal (green bars).

The second-order susceptibility as a function of the nanocrystal size and copper-impurity content was calculated and was plotted in Fig. 4. As can be seen, the susceptibility increases with decreasing crystal size. It also shows that with increasing impurity content up to ~0.6% it significantly increased and with a further increase it decreased. However, the impurity dependence for a nanocrystal displays a fashion which can be modelled by a Gaussian-type function.

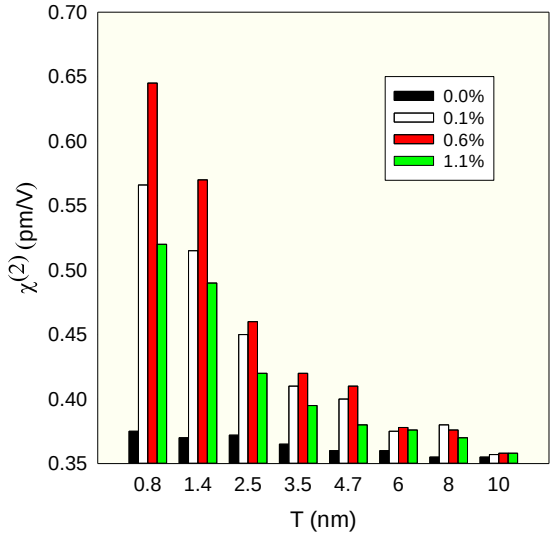

Fig.4: Second-order susceptibility as a function of the size and impurity content of the crystals. The background signal is for the intrinsic crystal (black bars).

Figure 5 shows the second-order susceptibility as a function of the size of thick crystals. As can be seen, the susceptibility for the crystal sizes larger than T = 250 nm gives the value at the background level (0.355 pm/V). Therefore, the size T > 250 nm may be identified as the bulk here. Bulk and intrinsic crystals show no considerable second harmonic effect.

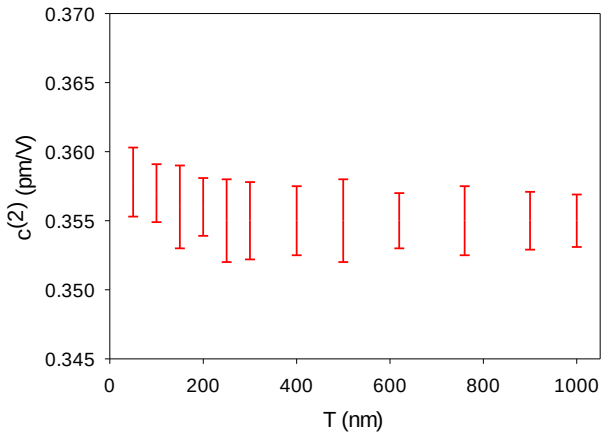

Fig. 5: Second-order susceptibility as a function of the size of thick crystals (with impurity content of 0.6%). Bars show the deviations from the average.

The insertion of the impurities favours a stronger local electron-phonon interaction, particularly its anharmonic part, through the alignment of the local anharmonic dipole moments by the pumping light [17]. Since the local electron-phonon anharmonicity is described by third-order rank tensor in disordered systems, the second harmonic is very similar to that one introduced for the third-order nonlinear optical susceptibility. It has been confirmed by observing the large photoluminescent yield of the intrinsic CdI_2 crystals [18], where the photoluminescence dependence was around three orders of magnitude in power density indicating that the nonlinear response is due to a third-order process.

It can be seen that the second-order susceptibility decreases for relatively higher impurity content, and for the concentration higher than ~1% it reduces almost to that of the intrinsic or pure CdI_2 crystals. This decrease of it with increasing impurity content are caused by aggregation of the copper impurities is typical of such kinds of layered crystals. This defect-assisted effect can be understood in terms of the impurity induced metallic-aggregators that formed in the process [5,7,19]. The formation of the metallic aggregators favours a reduction in the active electron–phonon centres, effectively contributing to the noncentrosymmetry of the output charge density as well as lead to the occurrence of metallic clusters which additionally scatter light, and consequently, suppresses the effect at higher impurity content through the limitation of the enhancement of the local hyperpolarizability for the aggregators as well as the corresponding nonlinear dielectric susceptibility [20,21].

Thinner nanocrystals are also found to significantly enhance the effect inducing the noncentrosymmetricity in the crystals. The larger surface-to-volume ratio of the nanomaterial plays an important role in the observed effect,

as the SHG probes the surface effects of the material. Here, in these optical processes, quantum confinement dominates the material's optical properties [22,23]. The nanometer-sized crystals or nanocrystals take into account the nano-sized quantum-confined effect or nano-confined effect, where *k*-space bulk-like dispersion disappears and discrete excitonic-like nanolevels occur within the forbidden energy gap of the manomaterial exhibiting optical nonlinearities [24,25].

4. Conclusions

Cadmium iodide nanocrystals were investigated using a pump-probe experiment. The experiment probed the doubled-frequency SHG. The second–order optical susceptibility was calculated from the experimentally measured SHG data. A significant increase of the optical susceptibility was achieved. However, bulk and pure crystals showed no considerable SHG effect. The observed results demonstrated the copper doping and nano-sized quantum-confinement effects in optical susceptibility in the materials. The results were discussed on the basis of the impurity induced metallic-aggregators and photoinduced electron-phonon anharmonic interactions.

Conflicts of Interest

The author has no conflicts of interest.

References

[1] Haug, H.,1988. Optical Nonlinearities and Instabilities in Semiconductors, Academic press, New York.
[2] Miah, M. I., 2001. Determination of multiphoton absorption coefficient of cadmium iodide using nonlinear transmittance and photoluminescence methods. Optical Materials, 18, p.231.
[3] Miah, M. I., 2009. Two-photon spin-polarization spectroscopy in Si-doped GaAs, Journal of Physical Chemistry B, 113, p.6800
[4] Miah, M. I. and Kasperczyk, J., 2009. Cu-doping effects in CdI_2 layered nanostructures: the role of photo-induced electron-phonon anharmonic interactions, Applied Physics Letters, 94, p. 053117.
[5] Cazzanelli, M. and Schilling, J., 2016. Second order optical nonlinearity in silicon by symmetry breaking. Applied Physics Reviews, 3, p.011104.
[6] Miah, M. I., 2009. Impurity–defect induced noncentrosymmetricity in nonlinear optical processes. Materials Chemistry and Physics, 118, p.417.
[7] Kityk, I. V., Pyroha, S. A., Mydlarz, T., Kasperczyk, J. and Czerwinski, M., 1998. Magnetic field induced ferroelectricity in copper doped CdI_2 single crystals, Ferroelectrics, 205, p.107.
[8] Miah, M. I., 2019. Induction strategies of the noncentrosymmetricity in centrosymmetric nonlinear optical nanocrystal processes. The European Physical Journal B, 92, p.224.
[9] Bordas, J., Robertson, J., Jakobsson, A., 1978. Ultraviolet properties and band structure of SnS_2, $SnSe_2$, CdI_2, PbI_2, BiI_2 and BiOI crystals. Journal of Physics C, 11, p.2607.
[10] Nakagawa, H. and Kitaura, M., 1995. Optical nonlinear processes. Proceedings SPIE, 2362, p.294.
[11] Robertson, J., 1979. Electronic structures of SnS_2, $SnSe_2$, CdI_2, PbI2. Journal of Physics C, 12, p.4753.
[12] Slater, J. C., 1956. Barrier theory of the photoconductivity of lead sulfide. Physical Review, 103, p.1631.
[13] Mott, N.F. and Davis, E. A., 1979. Electronic processes in non-crystalline Materials, Clarendon Press, Oxford.
[14] Herest, D and Voolless, F., 2004. Manifestation of nano-sized effects in photoinduced nonlinear optics of CdI2-Cu layered single crystals. Optics and Laser Engineering, 42, p.85.
[15] Bridgman, P.W., 1952. The Resistance of 72 Elements, Alloys and Compounds to 100,000 Kg/Cm². Proceedings of American Academy of Arts and Sciences, 81, p.165.
[16] Miah, M. I., 2021. Size- and temperature-control optical direct/indirect band tuning in layered compounds: band gap engineering, Optical and Quantum Electronics, 53, p. 618.
[17] Barbagiovanni, *E. G.*, Lockwood, D. J., Simpson, P.J. and Goncharova, L. V., 2014. Quantum confinement in Si and Ge nanostructures: Theory and experiment. Applied Physics Reviews, 1, p.011302.
[18] Miah, M. I., 2018. Multiphoton excitation and thermal activation in indirect bandgap semiconductors. Optical and Quantum Electronics, 50(9), p.355.
[19] Miah, M. I., 2009. Three-photon excited PL spectroscopy and photo-generated Frenkel defects in wide-bandgap CdI2 semiconductors. Physics Letters A, 374, p.75.
[20] Adduci, F., Cingolani, A., Ferrara, R., Lugara, M. and Minafra, M., 1977. High excitation intensity effects at different pump wavelengths in PbI2. Nuova Cimento B, 38, p.610.
[21] Catalano, I. M., Cingolani, A., Ferrara, R. and Lepore, M.,1985. Optical processes in layerd semiconductors. Helv. Physica Acta, 58, p.329.
[22] Khlebtsov, N. G., Trachuk, L. A. and Mel'nikov, A. G., 2005. Depolarization of light scattered by gold nanospheres and nanorods. Optics and Spectroscopy, 98, p.77.
[23] Zhanga, F., Xua, N., Zhao, J., Wang, Y., Jiang, X., Zhang, Y., Huang, W., Hu, L., Tang, Y., Xu, S. and Zhang, H., 2020. Two-dimensional materials for photonic applications. Nanophotonics, 9, p.1963.
[24] Edvinsson, T., 2018. Optical quantum confinement and photocatalytic properties in two, one- and zero-dimensional nanostructures. Royal Society Open.Science, 5, p.180387.
[25] Gopalan, V., Sanford, N. A., Aust, J. A., Kitamura, K. and Furukawa, Y., 2007. Crystal Growth, Characterization, and Domain Studies in Lithium Niobate and Lithium Tantalate Ferroelectrics, In: Handbook of Advanced Electronic and Photonic Materials and Devices, (Edited by H. S. Nalwa*)*, Vol. 4, Chapter 2, pp. 58-112, Elsevier.